GDCh

Communications

Angewandte
Chemie
International Edition
www.angewandte.org

VIP **Ribozymes** *Very Important Paper*

Ribozyme-Catalyzed Late-Stage Functionalization and Fluorogenic Labeling of RNA

*Carolin P. M. Scheitl, Takumi Okuda, Juliane Adelmann, and Claudia Höbartner**

Abstract: Site-specific introduction of bioorthogonal handles into RNAs is in high demand for decorating RNAs with fluorophores, affinity labels or other modifications. Aldehydes represent attractive functional groups for post-synthetic bioconjugation reactions. Here, we report a ribozyme-based method for the synthesis of aldehyde-functionalized RNA by directly converting a purine nucleobase. Using the methyltransferase ribozyme MTR1 as an alkyltransferase, the reaction is initiated by site-specific *N*1 benzylation of purine, followed by nucleophilic ring opening and spontaneous hydrolysis under mild conditions to yield a 5-amino-4-formylimidazole residue in good yields. The modified nucleotide is accessible to aldehyde-reactive probes, as demonstrated by the conjugation of biotin or fluorescent dyes to short synthetic RNAs and tRNA transcripts. Upon fluorogenic condensation with a 2,3,3-trimethylindole, a novel hemicyanine chromophore was generated directly on the RNA. This work expands the MTR1 ribozyme's area of application from a methyltransferase to a tool for site-specific late-stage functionalization of RNA.

Site-specific modifications of biomolecules for labeling and crosslinking have become increasingly important for studying structures, functions and interactions of nucleic acids[1] and proteins.[2] Among such modifications, aldehydes are attractive functional groups for bioconjugation, mostly by reaction with nitrogen nucleophiles through condensation or reductive amination.[3] Masked aldehydes can be installed synthetically, e.g. by solid-phase synthesis[4] or enzymatic

primer extension,[5] and released by deprotection of acetals, or generated by oxidative cleavage of 1,2-diols[6] or furan residues.[7] Alternatively, site-specific enzymatic transformations of amino acids or modified nucleotides can give rise to aldehyde functional groups for postsynthetic modification and bioconjugation with aldehyde reactive probes. For example, in DNA, aldehydes are introduced through the local generation of abasic sites that are in equilibrium with the open aldehyde form (Figure 1a), e.g. by uracil deglycosylase (UDG) or other lyases.[8] Natural modified nucleotides containing aldehyde functional groups such as 5-formylcytidine (f[5]C), are generated enzymatically by Fe[II]/α-ketoglutarate-dependent dioxygenases, e.g. TET enzymes[9] or ALKBH1[10] (Figure 1b). In proteins, internal site-specific generation of an aldehyde side chain has been described by formylglycine generating enzyme (FGE), which oxidizes a cysteine in a specific sequence context (Figure 1c).[11] The
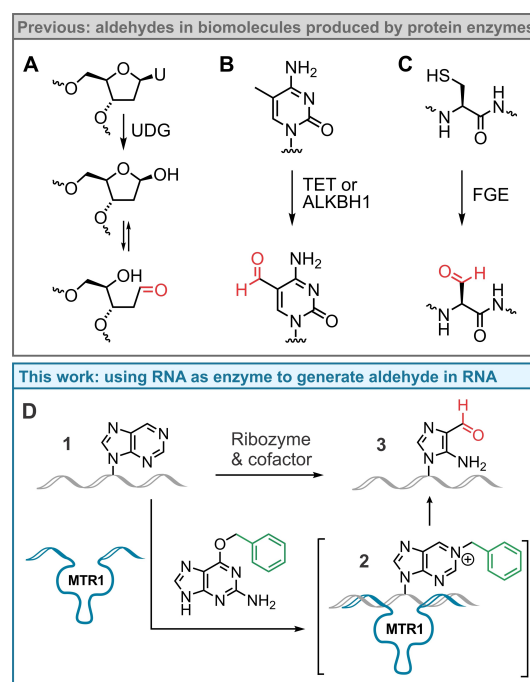
[*] C. P. M. Scheitl, Dr. T. Okuda, Dr. J. Adelmann,
Prof. Dr. C. Höbartner
Julius-Maximilians-Universität Würzburg, Institute of Organic
Chemistry
Am Hubland, 97074 Würzburg (Germany)
E-mail: claudia.hoebartner@uni-wuerzburg.de

Prof. Dr. C. Höbartner
Julius-Maximilians-Universität Würzburg, Center for Nanosystems
Chemistry
Theodor-Boveri-Weg, 97074 Würzburg (Germany)

Figure 1. Enzymatic generation of aldehydes in nucleic acids and proteins. A) Formation of abasic site in DNA by glycosylases (e.g. UDG). B) Oxidation of m[5]C to f[5]C in DNA/RNA by dioxygenase enzymes of the AlkB family (e.g. TET in DNA or ALKBH1 in tRNA). C) Oxidation of cysteine to formylglycine in a peptide tag consensus motif (CxPxR) by formylglycine-generating enzyme (FGE). D) RNA-catalyzed synthesis of 5-amino-4-formylimidazole nucleobase analogue **3** in RNA via *N*1 benzylation of a specific purine nucleobase.

aldehyde-tag[12] is used as short genetically encoded peptide tag that is fused to a protein of interest, and after treatment with FGE the resulting formylglycine is further chemically modified. Here, we developed a conceptually similar modification strategy for RNA that employs a synthetic ribozyme as a mimic of an aldehyde generating enzyme. A purine nucleobase (**1**) in RNA is converted to a 4-formylimidazolyl nucleoside analogue (**3**) in a site-specific manner, enabled by an RNA-alkylating ribozyme that generates 1-benzylpurine (**2**) as an intermediate (Figure 1d).

The aldehyde generation in RNA is enabled by our recently reported methyltransferase ribozyme MTR1,[13] which catalyzes the methylation of adenosine (A) at the $N1$ position using O^6-methylguanine (m^6G) as the methyl group donor. Crystal structures revealed the mechanism of the MTR1 ribozyme,[14] which originated from an in vitro selection using biotinylated benzylguanine as alkyl group donor.[13] Thus, MTR1 is also an active alkyltransferase ribozyme with O^6-benzylguanine (Bn^6G) as the cofactor. Regarding the substrate scope of RNA-catalyzed RNA methylation by MTR1, previous atomic mutagenesis studies revealed that besides adenosine (A), $2'$-deoxyadenosine (dA), $2'$-O-methyladenosine (Am), 3-deazaadenosine (c^3A) and 7-deazaadenosine (c^7A) were tolerated as target nucleosides, while 2-aminopurine (2AP) and purine ribosides (i.e., Nebularine, Ne) did not show any shifted product bands on denaturing PAGE. More detailed analyses of the reaction products formed with Bn^6G by HPLC and ESI-MS revealed that the Ne-containing RNA was not unchanged. We studied the formation of the new product in detail and turned it into a useful RNA labeling approach that involves the formation of the aminoimidazole carbaldehyde **3**.

MTR1-catalyzed benzylation of unmodified RNA (i.e. containing adenosine at the target position) showed a single product corresponding to 1-benzyladenosine, which was detected by denaturing PAGE and anion-exchange HPLC, while RNAs that contained 2-aminopurine or 2,6-diaminopurine at the target site were unreactive (Figure S1). In contrast, when adenosine was replaced by nebularine, anion exchange HPLC of the reaction product showed an additional later eluting peak (Figure 2a), with increasing intensity after longer reaction time. The new product was lighter by nine mass units than the untreated Ne-RNA, suggesting that the purine ring was opened by nucleophilic attack of water, followed by hydrolysis of imine and formamide intermediates to generate the 5-amino-4-formyl-imidazol-1-yl riboside **3** in the otherwise intact RNA. The suggested mechanism is depicted in Figure S2 and supported by the detection of several partially hydrolyzed reaction intermediates by mass spectrometry. Nucleophilic ring opening of $N1$-alkylated purine nucleotides occurs in the context of the Dimroth rearrangement, which converts $N1$-alkylated to N^6-alkylated adenosines.[15] On the nucleoside level, similar ring-opening of $N1$-alkylated inosine and other purine nucleosides has been used synthetically, e.g. during atomic mutagenesis and for isotope-labeled nucleosides,[16] and other modifications.[17] However, the reaction mediated by MTR1 is the first observation of 5-aminoimidazole-4-carbaldehyde generation in an intact RNA oligonucleotide.
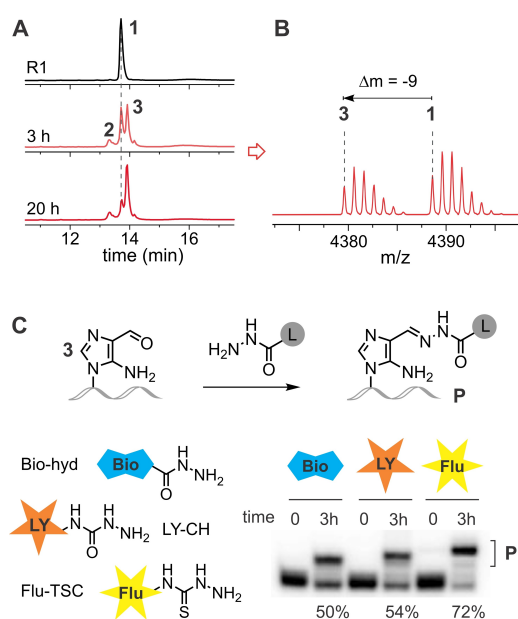

Figure 2. A) Anion-exchange HPLC monitored by UV absorbance at 260 nm of a 14-nt long nebularine-containing RNA R1 after incubation with MTR1 and Bn^6G for 3 h or 20 h at 25 °C, in MES buffer pH 6.0. B) Deconvoluted HR-ESI-MS spectrum of RNA isolated after 3 h shows formation of a product that has lost 9 mass units (mol wt. of R1 calculated. 4388.63 Da, found for the new product **3**: 4379.61 Da). C) Bioconjugation to aldehyde-reactive probes carrying various labels (L): Biotin (Bio) hydrazide (hyd), Lucifer Yellow (LY) carbohydrazide (CH) or fluorescein (Flu) thiosemicarbazide (TSC). N,N-dimethylethylenediamine at pH 7.5, 37 °C, 3 h, 20 % denaturing PAGE using $5'$-^{32}P-labeled RNA.

This newly generated internal formyl group in RNA is accessible for labeling with aldehyde reactive probes. We used biotin-hydrazide (Bio-hyd), Lucifer Yellow carbohydrazide (LY-CH) and fluorescein thiosemicarbazide (Flu-TSC) and optimized the reaction conditions by varying pH and buffer composition. N,N-dimethylethylenediamine (N,N-DMED)[18] buffer at pH 7.5 resulted in yields up to 72 % (Figure 1c), while other buffers gave only moderate conversion (Figure S3). These results establish the MTR1-mediated aldehyde unmasking of Ne-RNA as a potent tool for internal RNA labeling at physiological pH.

Building upon previous work on fluorogenic labeling of 5-formylpyrimidines,[19] we hypothesized that a new hemicyanine chromophore could possibly be generated in RNA containing the aldehyde nucleobase **3**. We examined the reaction with N-ethyl-2,3,3-trimethylindolenium-5-sulfonate (**4**) under various conditions and saw efficient formation of a new product band on PAGE (Figure 3 a,b). High-resolution ESI-MS analysis of the isolated full-length RNA product confirmed the expected condensation product in the RNA oligonucleotide with a monoisotopic mass of 4628.7 Da (Figure 3c). For further analysis, the isolated RNA was enzymatically digested and dephosphorylated to mononucleosides and analyzed by LC-MS. The new nucleoside was readily detected in the UV trace at 260 nm and in the extracted ion chromatogram (Figure 3d).[20] Thus, ESI-MS and LC-MS suggested that only one product was formed.
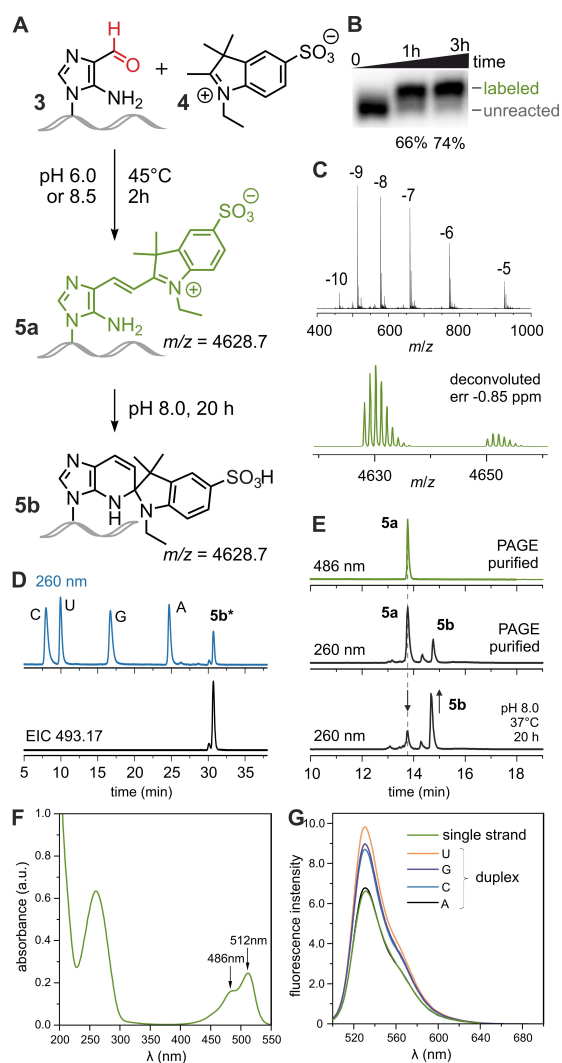
Figure 3. A) Fluorophore synthesis on RNA by condensation of **3** and **4**. The hemicyanine **5 a** can undergo spirocyclization to **5 b**. B) Gel image of RNA R1 containing **3** reacted with 75 mM **4** at pH 6.0 and 45 °C. C) Negative mode HR-ESI-MS (top) and deconvoluted spectrum (bottom) of the isolated product after reaction at pH 8.5 ($\Delta m = 22$, Na$^+$ salt). D) LC–MS analysis of digested isolated RNA from reaction with **4** at pH 8.5. UV traces at 260 nm (blue, individual nucleosides) and extracted ion chromatogram (EIC) corresponding to the modified nucleoside, marked by asterisk (**5 b***) (m/z ($M+H^+$) = 493.17 ± 0.01, for C$_{22}$H$_{28}$N$_4$O$_7$S). E) Anion-exchange HPLC of freshly isolated RNA with detection at 260 nm and 486 nm, and re-analysis after 20 h of incubation at pH 8, 37 °C (bottom). F) UV/Vis absorption spectrum of freshly isolated RNA (5 μM) showing absorption of **5 a** in the visible spectral range. G) Fluorescence emission spectra of RNA containing **5 a** as single strand, or hybridized to a complementary strand, containing either A, C, G, or U opposite to the chromophore (λ_{ex} = 486 nm).

Surprisingly, anion exchange HPLC of the full-length RNA isolated from the reaction at pH 8.5 showed two product peaks **5 a** and **5 b**. Only **5 a** showed absorbance at 486 nm, suggesting that **5 b** is an isomer likely formed by spirocyclization. Longer incubation in aqueous buffered solution increased the intensity of **5 b** (Figure 3e). In contrast to spiropyran photoswitches,[21] which can undergo ring-open-

ing to the merocyanine form even when incorporated into DNA,[22] in our preliminary screening we did not find conditions for efficient photochemical or thermal restoration of **5 a**. For characterizing the open hemicyanine **5 a** by optical spectroscopy, we used freshly PAGE-purified RNA that contained less than 20 % cyclized isomer. The UV/Vis absorption spectrum of freshly purified modified RNA revealed an absorption maximum at 512 nm and a shoulder at 486 nm (Figure 3f). Fluorescence emission upon excitation at 486 nm showed an emission maximum at 531 nm in both single- and double-stranded RNAs. The emission intensity was sensitive to the nucleoside facing **5 a** in the duplex. With adenosine, the duplex showed the same emission intensity as the single strand, while C, G, or U in the duplex opposite to **5 a** showed up to 50 % enhanced emission (Figure 3g). Given the promise for fluorogenic labeling of RNA, the reaction conditions were optimized to allow ribozyme-catalyzed alkylation, aldehyde generation and labeling to occur in one pot without the isolation of intermediates (Figure S4).

For general application of the RNA-catalyzed labeling strategy, facile accessibility of Ne-containing RNA is required. Although the nebularine phosphoramidite is commercially available, solid-phase synthesis is limited to rather short RNAs. These can be integrated into larger RNAs by enzymatic ligation.[23] Alternatively, in vitro transcription provides direct access to long RNAs, but modified nucleotides cannot easily be introduced site-specifically. However, even if nebularine was randomly incorporated during in vitro transcription by T7 RNA polymerase, the MTR1 ribozyme can be used to precisely select one position for derivatization, and this is achieved by appropriate design of the binding arms. It has been reported that 2′-deoxynebularine acts as an analogue of adenosine in DNA and predominantly forms base pairs with thymidine.[24] Nebularine has also been used during nucleotide analogue interference mapping (NAIM) of RNA, which requires its incorporation during in vitro transcription.[25] Thus, when ATP was replaced by NeTP (Figure 4a) during in vitro transcription of the 19-nt RNA Tr1, T7 RNA polymerase was able to generate a full-length product, which contained a single Ne nucleoside, as shown by HR-ESI-MS analysis and by LC-MS after digestion (Figure S7). Transcription yields were comparable to unmodified RNAs, and only dropped for consecutive nebularines, or when Ne was close to the transcription start site. MTR1-catalyzed conversion of Ne in the transcript and labeling of the generated aldehyde were similar to the synthetic RNAs made by solid-phase synthesis (Figure 4b,c). Importantly, we showed that MTR1 can site-specifically modify only the desired position in a transcript RNA that contained more than one nebularine, even if these are at neighbouring positions. This was confirmed by RNase T1 digestion and alkaline hydrolysis as shown in Figure 4d. A nebularine-guanosine mismatch in the ribozyme binding arm reduced the labeling efficiency, but good reaction yield could be restored by placing uridine across Ne in the binding arm (Figure S7).

Next, we moved to longer RNAs and chose in vitro transcribed tRNAs as substrates, which have previously
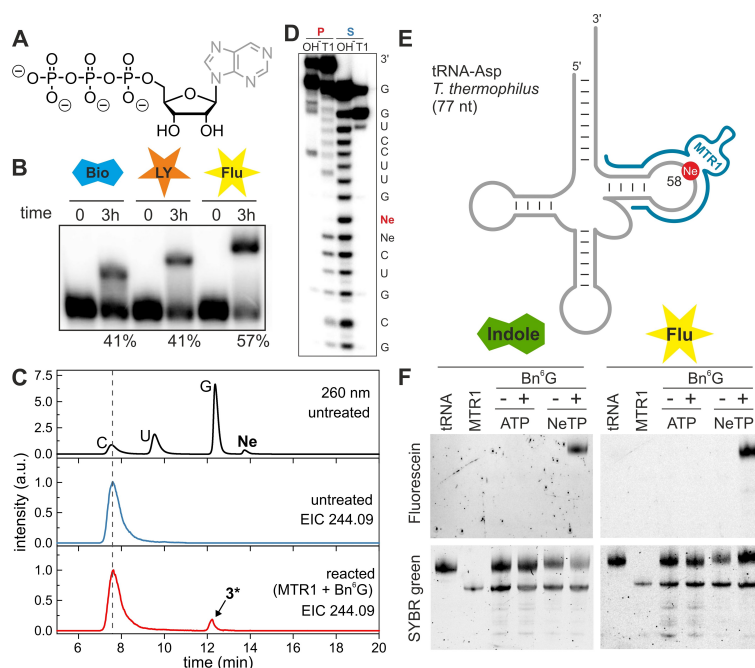
Figure 4. MTR1-catalyzed labeling of in vitro transcribed nebularine containing RNA. A) Structure of NeTP. B) Aldehyde generation and labeling of transcribed RNA Ne-Tr1 (19 nt). C) LC–MS analysis of digested unreacted and reacted (MTR1 + Bn⁶G treated) Ne-Tr1. UV trace at 260 nm and EIC (m/z 244.09 ± 0.01; note that **3** is a constitutional isomer of cytidine with the same sum formula $C_9H_{13}N_3O_5$). D) RNase T1 digestion and alkaline hydrolysis of untreated (substrate, S) or MTR1-modified and consecutively Flu-TSC labeled (product, P) transcript Ne-Tr2 (19 nt) with two consecutive Ne, of which only the desired one (marked in red) was modified site-specifically. E) Schematic representation of the labeling site at position 58 in *T. thermophilus* tRNA-Asp. F) *T. thermophilus* tRNA-Asp was transcribed using ATP or NeTP, treated with MTR1 in the presence (+) or absence (−) of Bn⁶G followed by conjugation with **4** or Flu-TSC. The gels were imaged in the fluorescein-channel (top) to detect the labeled RNAs, and then stained with SYBR green (bottom) to visualize tRNA and MTR1.

been shown to be accessible for MTR1-catalyzed installation of m¹A.[13] The *Thermus thermophilus* tRNA-Asp was transcribed in the presence of NeTP, and modified by an MTR1 ribozyme targeting position 58 (Figure 4e). Successful generation of **3** in tRNA was revealed by the presence of a strongly fluorescent band upon conjugation to Flu-TSC, while no fluorescence was detected in the negative control reactions (Figure 4f). Similarly, generation of fluorophore **5** allowed for selective visualization of the tRNA (Figure 4f).

In summary, we report the site-specific generation of a formylimidazole nucleotide analogue in RNA initiated by an alkyltransferase ribozyme. Using O^6-benzylguanine as the small molecule cofactor, the MTR1 ribozyme alkylates nebularine to generate 5-amino-4-formylimidazole-ribonucleoside at a specific internal position in the target RNA. The aldehyde can easily be further conjugated with various nucleophiles. We demonstrated the versatility of this approach by fluorescent labeling of a full-length tRNA transcript. In addition, through condensation of the 5-aminoimidazole-4-carbaldehyde **3** with a 2,3,3-trimethylindole moiety, we generated a novel environmentally sensitive hemicyanine fluorophore directly on the RNA. This reaction opens the possibility to synthesize alternative chromophores with altered fluorescent properties that could serve as probes for elucidating nucleic acid structures and dynamics. Furthermore, the MTR1-ribozyme catalyzed aldehyde generation holds potential for nucleic acid-protein

crosslinking[26] via nucleophilic amino acid side chains to covalently trap proteins that are associated with their DNA or RNA targets. Overall, this work establishes nebularine as aldehyde precursor in RNA and demonstrates its post-synthetic functionalization by an alkyltransferase ribozyme, thus expanding the ribozyme toolbox for RNA labeling.[27]

Supporting Information

Experimental procedures, analytical NMR and MS data, supplementary Figures.

Acknowledgements

Conflict of Interest

The authors declare no conflict of interest.

Data Availability Statement

[1] a) N. Klöcker, F. P. Weissenboeck, A. Rentmeister, *Chem. Soc. Rev.* **2020**, *49*, 8749–8773; b) R. Micura, C. Höbartner, *Chem. Soc. Rev.* **2020**, *49*, 7331–7353; c) H. Depmeier, E. Hoffmann, L. Bornewasser, S. Kath-Schorr, *ChemBioChem* **2021**, *22*, 2826–2847; d) M. Flamme, L. K. McKenzie, I. Sarac, M. Hollenstein, *Methods* **2019**, *161*, 64–82.

[2] a) G. Zhang, S. Zheng, H. Liu, P. R. Chen, *Chem. Soc. Rev.* **2015**, *44*, 3405–3417; b) C. D. Spicer, B. G. Davis, *Nat. Commun.* **2014**, *5*, 4740; c) T. A. Nguyen, M. Cigler, K. Lang, *Angew. Chem. Int. Ed.* **2018**, *57*, 14350–14361.

[3] a) J. Kalia, R. T. Raines, *Curr. Org. Chem.* **2010**, *14*, 138–147; b) D. K. Kölmel, E. T. Kool, *Chem. Rev.* **2017**, *117*, 10358–10376.

[4] a) A. Okamoto, K. Tainaka, I. Saito, *Tetrahedron Lett.* **2002**, *43*, 4581–4583; b) Q. Dai, C. A. He, *Org. Lett.* **2011**, *13*, 3446–3449; c) K. Sato, W. Hirose, A. Matsuda, *Current Protocols in Nucleic Acid Chemistry*, Wiley, Hoboken, **2008**, chap. 1, Unit 1 21; d) M. Münzel, U. Lischke, D. Stathis, T. Pfaffeneder, F. A. Gnerlich, C. A. Deiml, S. C. Koch, K. Karaghiosoff, T. Carell, *Chem. Eur. J.* **2011**, *17*, 13782–13788.

[5] a) V. Raindlová, R. Pohl, M. Šanda, M. Hocek, *Angew. Chem. Int. Ed.* **2010**, *49*, 1064–1066; b) M. M. Krömer, M. Brunderová, I. Ivancová, L. Poštová Slavětínská, M. Hocek, *ChemPlusChem* **2020**, *85*, 1164–1170.

[6] a) C. T. Wirges, J. Timper, M. Fischler, A. S. Sologubenko, J. Mayer, U. Simon, T. Carell, *Angew. Chem. Int. Ed.* **2009**, *48*, 219–223; b) S. Mukherjee, A. Guainazzi, O. D. Schärer, *Nucleic Acids Res.* **2014**, *42*, 7429–7435; c) A. S. Romanenkov, A. A. Ustyugov, T. S. Zatsepin, A. A. Nikulova, I. V. Kolesnikov, V. G. Metelev, T. S. Oretskaya, E. A. Kubareva, *Biochemistry* **2005**, *70*, 1212–1222; d) V. L. Tunitskaya, E. E. Rusakova, L. V. Memelova, S. N. Kochetkov, A. Van Aerschot, et al., *FEBS Lett.* **1999**, *442*, 20–24; e) M. Krömer, K. Bártová, V. Raindlová, M. Hocek, *Chem. Eur. J.* **2018**, *24*, 11890–11894.

[7] a) L. L. Carrette, E. Gyssels, J. Loncke, A. Madder, *Org. Biomol. Chem.* **2014**, *12*, 931–935; b) L. L. Carrette, T. Morii, A. Madder, *Bioconjugate Chem.* **2013**, *24*, 2008–2014.

[8] a) J. A. Wilde, P. H. Bolton, A. Mazumder, M. Manoharan, J. A. Gerlt, *J. Am. Chem. Soc.* **1989**, *111*, 1894–1896; b) J. J. Vasseur, D. Peoch, B. Rayner, J. L. Imbach, *Nucleosides Nucleotides* **1991**, *10*, 107–117.

[9] T. Pfaffeneder, B. Hackner, M. Truss, M. Münzel, M. Müller, C. A. Deiml, C. Hagemeier, T. Carell, *Angew. Chem. Int. Ed.* **2011**, *50*, 7008–7012.

[10] S. Haag, K. E. Sloan, N. Ranjan, A. S. Warda, J. Kretschmer, C. Blessing, B. Hubner, J. Seikowski, S. Dennerlein, P. Rehling, M. V. Rodnina, C. Höbartner, M. T. Bohnsack, *EMBO J.* **2016**, *35*, 2104–2119.

[11] I. S. Carrico, B. L. Carlson, C. R. Bertozzi, *Nat. Chem. Biol.* **2007**, *3*, 321–322.

[12] D. Rabuka, J. S. Rush, G. W. deHart, P. Wu, C. R. Bertozzi, *Nat. Protoc.* **2012**, *7*, 1052–1067.

[13] C. P. M. Scheitl, M. Ghaem Maghami, A. K. Lenz, C. Höbartner, *Nature* **2020**, *587*, 663–667.

[14] a) C. P. M. Scheitl, M. Mieczkowski, H. Schindelin, C. Höbartner, *Nat. Chem. Biol.* **2022**, *18*, 547–555; b) J. Deng, T. J. Wilson, J. Wang, X. Peng, M. Li, X. Lin, W. Liao, D. M. J. Lilley, L. Huang, *Nat. Chem. Biol.* **2022**, *18*, 556–564.

[15] a) J. B. Macon, R. Wolfenden, *Biochemistry* **1968**, *7*, 3453–3458; b) H. Liu, T. Zeng, C. He, V. H. Rawal, H. Zhou, B. C. Dickinson, *ACS Chem. Biol.* **2022**, *17*, 1334–1342.

[16] a) M. D. Erlacher, K. Lang, B. Wotzel, R. Rieder, R. Micura, N. Polacek, *J. Am. Chem. Soc.* **2006**, *128*, 4453–4459; b) S. Neuner, T. Santner, C. Kreutz, R. Micura, *Chem. Eur. J.* **2015**, *21*, 11634–11643.

[17] a) K. Leškovskis, J. M. Zaķis, I. Novosjolova, M. Turks, *Eur. J. Org. Chem.* **2021**, 5027–5052; b) S. Budow, F. Seela, *Chem. Biodiversity* **2010**, *7*, 2145–2190.

[18] D. Larsen, A. M. Kietrys, S. A. Clark, H. S. Park, A. Ekebergh, E. T. Kool, *Chem. Sci.* **2018**, *9*, 5252–5259.

[19] a) B. Samanta, J. Seikowski, C. Höbartner, *Angew. Chem. Int. Ed.* **2016**, *55*, 1912–1916; b) C. Liu, Y. Wang, W. Yang, F. Wu, W. Zeng, Z. Chen, J. Huang, G. Zou, X. Zhang, S. Wang, X. Weng, Z. Wu, Y. Zhou, X. Zhou, *Chem. Sci.* **2017**, *8*, 7443–7447; c) J. Dietzsch, D. Feineis, C. Höbartner, *FEBS Lett.* **2018**, *592*, 2032–2047; d) Y. Wang, X. Zhang, G. Zou, S. Peng, C. Liu, X. Zhou, *Acc. Chem. Res.* **2019**, *52*, 1016–1024.

[20] The long incubation conditions for digestion into mononucleotides by snake venom phosphodiesterase and dephosphorylation by bacterial alkaline phosphatase (pH 7.5, 37 °C, 20 h) promoted the spirocyclization to **5b**. See Supporting Information Figure S5 and S6 for the analysis of product distributions under varying pH and buffer conditions.

[21] a) T. Halbritter, C. Kaiser, J. Wachtveitl, A. Heckel, *J. Org. Chem.* **2017**, *82*, 8040–8047; b) J. Buback, P. Nuernberger, M. Kullmann, F. Langhojer, R. Schmidt, F. Würthner, T. Brixner, *J. Phys. Chem. A* **2011**, *115*, 3924–3935.

[22] C. Brieke, A. Heckel, *Chem. Eur. J.* **2013**, *19*, 15726–15734.

[23] a) J. Hertler, K. Slama, B. Schober, Z. Ozrendeci, V. Marchand, Y. Motorin, M. Helm, *Nucleic Acids Res.* **2022**, *50*, e115; b) C. Höbartner, R. Rieder, C. Kreutz, B. Puffer, K. Lang, et al., *J. Am. Chem. Soc.* **2005**, *127*, 12035–12045; c) T. P. Hoernes, K. Faserl, M. A. Juen, J. Kremser, C. Gasser, et al., *Nat. Commun.* **2018**, *9*, 4865.

[24] M. S. Rahman, M. Z. Humayun, *Mutat. Res.* **1997**, *377*, 263–268.

[25] S. P. Ryder, S. A. Strobel, *Methods* **1999**, *18*, 38–50.

[26] a) J. Nakamura, M. Nakamura, *DNA Repair* **2020**, *88*, 102806; b) S. S. Pujari, M. Wu, J. Thomforde, Z. A. Wang, C. Chao, N. M. Olson, L. Erber, W. C. K. Pomerantz, P. Cole, N. Y. Tretyakova, *Angew. Chem. Int. Ed.* **2021**, *60*, 26489–26494; c) V. Raindlová, R. Pohl, M. Hocek, *Chem. Eur. J.* **2012**, *18*, 4080–4087.

[27] a) M. Ghaem Maghami, C. P. M. Scheitl, C. Höbartner, *J. Am. Chem. Soc.* **2019**, *141*, 19546–19549; b) M. Ghaem Maghami, S. Dey, A. K. Lenz, C. Höbartner, *Angew. Chem. Int. Ed.* **2020**, *59*, 9335–9339.